

Experimental Investigation and Statistical Analysis of Creep Properties of a Hybridized Epoxy-Alumina-Calcium Silicate Nanocomposite Material Operating at Elevated Temperatures

Obuka Nnaemeka Sylvester P., Ihueze Chukwutoo Christopher, Okoli Ndubuisi Celestine, Ikwu Gracefield Okwudilichukwu R.

Abstract - The experiments of this research were designed to lend itself to two way and three way classification ANOVA analysis in the SPSS software. The new hybrid epoxy matrix composites consist of 5%wt, 10%wt, 15%wt, 20%wt, 25%wt, and 30%wt of fillers (alumina and calcium silicate) in nanoscale. Tensile strength of each constituent material was obtained through tensile experiments. Creep experiments were performed at temperatures of 50°C, 70°C, 90°C, 110°C, and 130°C, at constant loading of 14 MPa. The composite material with 15%wt constituent showed highest tensile strength followed by the 20%wt constituent showing higher strength than a baseline Epoxy-Alumina nanocomposite. Also the 15%wt and the 20%wt constituents exhibited the best resistant property to creep than every other constituent at short term creep tests and at analytical results. Though the two way classification ANOVA show enough significance at 95% confidence interval, the three way classification ANOVA showed significances of time, temperature and samples (with interactions), which are responsible for the creep failure of the studied composites. The creep limit property of the new material was found to be higher than the creep limit of the Epoxy filled with Alumina only.

Keywords: Nanocomposites, Epoxy, Alumina, Calcium Silicate, ANOVA, Creep, Tensile Strength, SPSS Software

1 INTRODUCTION

THIS research is carried out to develop a polymer matrix hybrid nanocomposite material for oil and gas supply system through classical experimental design and application of trendy analytical tools to investigate the materials' creep properties. The tests are carried out based on the maximum parameters of operation of oil and gas pipelines, basically temperature, pressure and corrosive environment (Seawater, H₂S and CO₂). Creep phenomenon is a natural failure mechanism for materials and equipments working under stress, high temperature and at a space of time. During high temperature services, components typically operate under complex non-steady stress-temperature conditions. Even so, the creep and creep fracture properties of engineering materials are usually determined under uniaxial tensile stresses, applying a known constant load to a specimen held at a fixed temperature (Wilshire and Evans, 1994).

Nanotechnology, nanostructured polymers, nanoparticles and nano composites have been a lot research topic of high promise for years. A lot has been done, highly interesting scientific findings and even significant technical applications, yet there are still significant unfulfilled promises and visions to be made true. It is good to keep in mind that nature is a master in optimizing nanostructures in materials. Also, nature has shown that significant improvements in materials properties can be reached, and tailored properties achieved (Seppala, 2010). Nanocomposite materials have emerged as suitable alternatives to overcome limitations of micro composites and monolithic, while posing preparation challenges related to the control of elemental composition and stoichiometry in the nano cluster phase. In 1995, the deep-water offshore oil industry was looking for strong, lightweight materials to replace the heavy alloy piping used on oil platform in seawater as was reported by Lea (2002), of Specialty Plastics Inc., by reducing the weight of the piping materials on the service deck of a Tension Leg Platform (TLP), the buoyancy of the TLP would increase. This would reduce the amount of structural steel needed below water, there by significantly reducing the cost of a TLP. Although carbon steel, copper-nickel alloy and duplex steel pipe had traditionally been used on offshore platforms and pipelines, advanced composite were known to be stronger, more resistant to corrosion, and lighter than steel. For example, composite pipe with a 6 inch diameter weighs 4 pounds per foot, while a copper nickel pipe with the same diameter weighs 24 pounds per foot. Advanced composites also cost less initially than steel piping and have a longer life cycle (Schmidt, Shah and Giannelis, 2002). Epoxy resin systems are increasingly used as matrix in composite materials for a wide range of automotive, aerospace, oil and gas applications and for ship building or electronic devices.

- Obuka Nnaemeka Sylvester P. is currently pursuing a doctor of philosophy degree program in Industrial/Production Engineering department at Nnamdi Azikiwe University, Awka, Nigeria. PH:+234(0)8034002623. E-mail: silvermek7777@yahoo.com
- Ihueze, Chukwutoo Christopher is a Professor of design and engineering management in Industrial/Production Engineering department at the same University as the corresponding author. Okoli Ndubuisi Celestine; and Ikwu Gracefield Okwudilichukwu R., are currently pursuing the same degree program as the corresponding author in the same department and in the same University.

Nano particles constrain the matrix deformation less than microparticles, because they integrate better into the polymer microstructure as they approach nearly molecular dimensions. Depending on more or less strong interactions with the matrix, it can be expected that they influence deformation mechanisms in the polymer on the micro or even the nano scale.

2 LITERATURE REVIEW

Nanoscale science and technology research is progressing with the use of a combination of atomic scale characterization and detailed modeling (Roy, Roy, and Roy, 1986). In the early 1990s, Toyota Central Research Laboratories in Japan reported work on a Nylon-6 nanocomposite (Usuki, et al, 1993), for which a very small amount of nano filler loading resulted in a pronounced improvement of thermal and mechanical properties. "The properties of nanocomposite materials depend not only on the properties of their individual parents (nano filler and nylon, in this case) but also on their morphology and interfacial characteristics", says Kanartzidis (Oriakhi, 1998). The transition from microparticles to nanoparticles yields dramatic changes in physical properties. Nanoscale materials have a large surface area for a given volume (Luo and Daniel, 2003). Since many important chemical and physical interactions are governed by surfaces and surface properties a nanostructured material can have substantially different properties from larger-dimensional materials of the same composition (RTO, 2005). In general, nanomaterials provide reinforcing efficiency because of their high aspect ratio. The properties of a nanocomposite are greatly influenced by the size scale of its component phases and the degree of mixing between the two phases. Depending on the nature of the components used (layered silicate or nanofiber, cation exchange capacity, and polymer matrix) and the method of preparation, significant differences in composite properties may be obtained (Park, et al, 2001). Analogously, in fibrous or particle reinforced Polymer Nanocomposites (PNC), dispersion of the nanoparticle and adhesion at the particle-matrix interface play crucial roles in determining the mechanical properties of the nanocomposite. Without proper dispersion, the nanomaterial will not offer improved mechanical properties over that of the conventional composites, in fact, a poorly dispersed nanomaterial may degrade the mechanical properties (Gorga and Cohen, 2004).

2.1 Potentials and Opportunities in Polymer-Nanocomposites

Polymers have been filled with several inorganic compounds, either synthetic or natural, in order to increase heat and impact resistance, flame retardancy and mechanical strength, and to decrease electrical conductivity and gas permeability with respect to oxygen and water vapour (Fischer, 2003). Furthermore, metal and ceramic reinforcements offer striking routes to certain unique magnetic, electronic, optical or catalytic properties coming from inorganic nano-particles, which add to other polymer properties such as processibility and film forming capability (Athawale, et al, 2003). Using this approach polymers can be improved while keeping their lightweight and ductile nature (Jordan, et al, 2005; Akita and Hatlori, 1999; Zavyalov, Pivkina, and Schoonman, 2002). Another

important aspect is that nanoscale reinforcements have an exceptional potential to generate new phenomena, which leads to special properties in these materials. It may be pointed out that the reinforcing efficiency of these composites, even at low volume fractions, is comparable to 40-50% for fibers in microcomposites (Ray and Bousmina, 2005). Addition of reinforcements to a wide variety of polymer resins produces a dramatic improvement in their biodegradability. For instance, rocket propellants are prepared from a Polymer-Al/Al₂O₃ nanocomposite to improve ballistic performance (Meda, et al, 2005). Thermosetting and thermoplastic pipes and liners created from nanocomposite materials have enhanced thermo-mechanical and creep properties, allowing for operations at higher temperatures and pressures without increasing the thickness of the pipe or changing the manufacturing processes involved (Vincenzo, Gasem, and Mauced, 2010). Drill bits coated with nanostructured ceramic materials have increased hardness and durability compared with their conventional counterparts (Milue, 2009). Another major area where nanocomposite materials can make a dramatic impact is with sealants. Currently used rubber sealants and O-rings are very stable under common well conditions (175°C and 135MPa), exhibiting appropriate flexibility and structural stability. When subjected to harsher conditions, however, the structural integrity of the rubber is severely compromised (Endo, Naguchi, and Ho, 2008). In high-temperature-pressure condition, old electrical sensors and other measuring tools often are not reliable. But researchers currently are developing a set of reliable and economical sensors from optical fibers for measuring temperature and pressure, oil flow-rate, and acoustic waves in oil wells (Scott, Jones and Crudden, 2003; Ying and Sun, 1997). Another nanosensor, Smart Dust, is being developed by researchers at the University of California in San Diego. Smart Dust was created from nanostructured porous silicon crystals that can be tuned to change colour when a specific compound is detected. Within the oil and gas industry this sort of technology could be deployed to remotely sense pipeline leaks for gases, such as toxic hydrogen sulphide, or to remotely monitor the structural integrity of pipelines and wells (Sailor and Link, 2005). Evora and Shukla (2003) have reported improvement in fracture toughness for polyester resin reinforced with TiO₂ nanoparticles; however the tensile strength of the composites was lower than that of the resin at higher particle volume fraction. Similar trend of reduction in tensile strength was reported by Daniel et al (2003) for epoxy-clay nanocomposites. Gojny, et al, (2004), achieved moderate improvements in fracture toughness and elastic modulus of epoxy by the addition of carbon nanotubes, but the tensile strength decreased when the nanotubes were used without any treatment. Yong and Hahn (2004) also have reported decrease in tensile strength for vinyl ester reinforced with unmodified SiC nanoparticles. While agglomeration of nanoparticles at higher volume fractions is one of the reasons attributed for decrease in the tensile strength. The more prominent reason is the lack of chemical bonding between the inorganic particles and organic matrix. Masahiro, et al, (2006), studied the preparation and various characteristics of Epoxy /Alumina nanocomposites by dispersing 3, 5, 7 and 10weight (wt)% boehmite alumina nanofillers in a bisphenol A epoxy resin using a special two-

stage direct mixing method. It was elucidated that nanofillers affect various characteristic of epoxy resins, when they are nano structured. Omrani, Simon and Rostami (2009), investigated the effect of alumina nanoparticle on the properties of an epoxy resin system. Formation of composite made up of alumina particles in gamma phase and diglycidyl ether of bisphenol-A, the following were observed: From the kinetic analysis using the Avrami equation, it has been seen that the kinetic parameters are influenced by the presence of nanoparticle and the used curing temperatures. It was found that a relatively low concentration of Al₂O₃ nanoparticles led to an impressive improvement of dynamic mechanical, mechanical, and thermal properties.

3 MATERIALS AND METHOD

The methodology of this research work on development of hybrid nanocomposite material is experimental and analytical employing mix-method approach. This hybrid polymer nanocomposite is made of Epoxy matrix, and two nano-fillers of Aluminum Oxide (Al₂O₃) and Calcium Silicate (CaSiO₃). Due to factor of availability, the combination system of Epikote Resin 836/Epikure curing Agent F205 is used in this research. About twelve (12) samples were produced, six(6) of which are the hybrid composites of 5 wt%, 10wt%, 15wt%, 20wt%, 25wt% and 30wt%, weight fractions of the fillers (fibre). The other six (6) samples will be used as baseline samples for the experiment made of epoxy-alumina nanocomposites of the same weight fractions of the filler (fibre) as in the hybrid nanocomposite samples. Hence the samples are labeled samples A, B, C, D,..... to L. The resin and its curing agent, which form the epoxy matrix were measured at the ratio of 2:1. Due to the application of the centrifugal force, the curing temperature of the composite is recorded at between 1800C and 1850C. The composite is allowed to cure at this temperature of $T \leq 1850C$ for 6 hours (360mins), after which it is allowed for post-cure at ambient temperature without external air cooling for at least 24 hours. Table 3 shows the dimension of the samples used in the experiment.

TABLE 1: DIMENSIONS OF TENSILE TEST SAMPLES

Specimen	Gage Length (mm)	Thickness (mm)	Width (mm)	Length of Grip section (mm)
A (5H)	60	7.5	15	20
B (10H)	60	9	15	20
C (15H)	60	7	15	20
D (20H)	60	8	15	20
E (25H)	60	6	15	20
F (30H)	60	6	15	20
G (5C)	60	9	15	20
H (10C)	60	7	15	20
I (15C)	60	8	15	20
J (20C)	60	8	15	20
K (25C)	60	7	15	20
L (30C)	60	7	15	20

3.1 Theory of Tensile Tests

If the results of tensile testing are to be used to predict how a metal will behave under other forms of loading, it is desirable to plot the data in terms of true stress and true strain. The measurement of elongation is used to calculate the engineering or nominal strain ϵ_n , using the following equation, (ASMI, 2011);

$$\epsilon_n = \frac{\Delta L}{L_0} = \frac{L_f - L_0}{L_0} \quad (1)$$

Engineering or nominal stress, σ_n , is defined as;

$$\sigma_n = F/A_0 \quad (2)$$

When force-elongation data are converted to engineering stress and strain, a stress-strain curve that is identical in shape to the force-elongation curve can be plotted. The advantage of dealing with stress versus strain rather than load versus elongation is that the stress-strain curve is virtually independent of specimen dimensions. However, true stress, σ , is defined as;

$$\sigma = F/A_f \quad (3)$$

where A_f is the cross sectional area at the time that the applied force is F. Up to the point at which necking starts, true strain, ϵ (natural or logarithmic), is defined as;

$$\epsilon = \ln \left(\frac{L_f}{L_0} \right) \quad (4)$$

This definition arises from taking an increment of the strain, $d\epsilon$, as the incremental change in length, dL , divided by the length, L , at the time, $d\epsilon = dL/L$, and integrating. As long as the deformation is uniform along the gage section, the true stress and strain can be calculated from the engineering quantities. With constant volume and uniform deformation, $L_f A_f = L_0 A_0$;

$$A_0/A_f = L_f/L_0 \quad (5)$$

Thus, according to equation (1);

$$A_0/A_f = 1 + \epsilon_n \quad (6)$$

Equation (3) can be rewritten as,

$$\sigma = \left(F/A_0 \right) \left(A_0/A_f \right) \quad (7)$$

and, with substitution of equations (2) and (6) into equation (7), we obtain;

$$\sigma = s (1 + \epsilon_n) \quad (8)$$

Substituting the expression $L_f/L_0 = 1 + \epsilon_n$ in accordance with equations (5) and (6), into the expression for true strain (4) gives the true strain as,

$$\epsilon = \ln (1 + \epsilon_n) \quad (9)$$

At very low strains, the differences between true and engineering stress and strain are very small. It does not really matter whether Young's modulus is defined in terms of engineering or true stress-strain. It must be emphasized that these expressions are valid only as long as the deformation is uniform. Once necking starts, equation (3) for true stress is still valid, but the cross-sectional area at the base of the neck must be measured directly rather than being inferred from the length measurements (Gedney, 2002). Because the true stress, thus calculated, is the true stress at the base of the neck, the corresponding true strain should also be at the base of the neck. Equation (4) could still be used if the L_f and L_0 values were known for an extremely short gage section centered on the middle of the neck (one so short that variations in area along it would be negligible). Of course, there will be no such gage section;

but if there were, equation (5) would be valid. Thus the true strain can be calculated as (Gedney, 2002);

$$\epsilon = \ln \left(\frac{A_0}{A_f} \right) \tag{10}$$

3.2 Material Strength (Tensile Tests)

The tensile strength (true stress) of each sample was obtained from equation (3), the cross-sectional area (Af) at the time that the applied force is F (see table 3) was calculated from a combination of equations (1) and (6). Assuming a uniform deformation at constant volume, the instantaneous area (Af) is also obtained through the application of equation (5). The original cross-sectional area (A0) of each sample's gage length domain (which is a prism) is given by the expression;

$$A_0 = 2 (L_0W + L_0h + Wh) \tag{11}$$

TABLE 2: SUMMARY OF TENSILE STRENGTH DATA

Sample	Original Area (A ₀)	Instantaneous Area (A _i)	Normal Strain (ε _n)	Force F (KN)	Tensile Strength (MPa)
A (5H)	.00029	.00027	0.090	13.25	49
B (10H)	.000315	.00029	0.103	17.30	59
C (15H)	.000285	.00028	0.077	25.20	84
D (20H)	.00030	.00028	0.087	23.68	90
E (25H)	.00027	.00025	0.063	19.00	63
F (30H)	.00027	.00025	0.060	13.40	54
G (5C)	.00032	.00030	0.087	12.00	40
H (10C)	.00029	.00026	0.117	13.00	50
I (15C)	.00030	.00028	0.087	15.10	54
J (20C)	.00030	.00029	0.103	18.52	64
K (25C)	.00029	.00027	0.090	19.40	72
L (30C)	.00029	.00027	0.087	22.40	83

4 THEORY OF DATA ANALYSIS USING ANOVA

4.1 Two Way Classification

The Two way classification model is expressed as;

$$X_{ijk} = \mu + \alpha_i + \beta_j + \lambda_{ij} + e_{ijk} \tag{12}$$

Where; α_i = Factor A effects

β_j = Factor B effects

λ_{ij} = (αβ)_{ij} = Interaction effects

The estimates of these parameters are;

$$\mu = \bar{X}_{..} \quad , \quad \alpha_i = \bar{X}_{i.} - \bar{X}_{..} \quad , \quad \lambda_{ij} = \bar{X}_{ij.} - \bar{X}_{i.} - \bar{X}_{.j} + \bar{X}_{..} \tag{13}$$

Where, $\bar{X}_{i.} = \frac{\sum_j T_{i.}^2}{q}$, $\bar{X}_{.j} = \frac{\sum_i T_{.j}^2}{p}$, $\bar{X}_{ij.} = \frac{\sum_{k=1}^r X_{ijk}}{q}$

And,

$$\bar{X}_{..} = \text{Grand mean}(\mu) = \frac{T_{...}}{pqr} \quad \text{as } T_{...} = \sum_{ijk} X_{ijk} \tag{14}$$

To test for the significance of the factors A, B, and interaction effects, we use the Two way ANOVA table proposed in table 3 (Eze, 2002);

TABLE 3: TWO WAY CLASSIFICATION ANOVA

Source of Variance	Degrees of Freedom	Sum of Squares	Mean Squares	F-ratio
Factor A	p-1	SSA	MSA	MSA/MS _e
Factor B	q-1	SSB	MSB	MSB/MS _e
Interaction (λ)	(p-1)(q-1)	SSλ	MΣλ	MΣλ/MS _e
Error	Pq(r-1)	SS _e	MS _e	
Total		SST		

Where; SSA = Sum of squares due to factor A

SSB = Sum of squares due to factor B

SSλ = Sum of squares due to interaction

MSA = Mean sum of squares due to factor A

MSB = Mean sum of squares due to factor B

MΣλ = Mean sum of squares due to interaction

The estimates of these parameters are;

$$SSA = C_i - C = \frac{\sum T_{i.}^2}{qr} = \frac{T_{...}^2}{pqr} \tag{15}$$

$$SSB = C_j - C = \frac{\sum T_{.j}^2}{pr} = \frac{T_{...}^2}{pqr} \tag{16}$$

$$SS\lambda = C_{ij} - C_i - C_j + C \tag{17}$$

Where, $C_{ij} = \frac{\sum T_{ij.}^2}{r}$

$$SSe = C_{ijk} - C_{ij} \tag{18}$$

Where, $C_{ijk} = \sum_{ijk} X_{ijk}^2$

$$MSA = \frac{SSA}{p-1} \tag{19}$$

$$MSB = \frac{SSB}{q-1} \tag{20}$$

$$M\Sigma\lambda = \frac{SS\lambda}{(p-1)(q-1)} \tag{21}$$

$$MSe = \frac{SSe}{pq(r-1)} \tag{22}$$

4.2 Three Way Classification

Three way classification relation is expressed classically as;

$$X_{ijkl} = \mu + \alpha_i + \beta_j + \lambda_k + (\alpha\beta)_{ij} + (\alpha\lambda)_{ik} + (\beta\lambda)_{jk} + (\alpha\beta\lambda)_{ijk} + e_{ijkl} \tag{23}$$

Where, α_i = Factor A effect

β_j = Factor B effect

λ_k = Factor C effect

(αβ)_{ij} = Interaction effect between A and B

(αλ)_{ik} = Interaction effect between A and C

(βλ)_{jk} = Interaction effect between B and C

(αβλ)_{ijk} = Interaction effect between A, B, and C

e_{ijkl} = Error or residual effect

The estimates for sum of squares of these parameters are;

$$SS\alpha_i = \frac{1}{ncl} \sum T_{i...}^2 - \frac{T_{...}^2}{N} \tag{24}$$

$$SS\beta_i = \frac{1}{nRL} \sum T_{.j.}^2 - \frac{T_{...}^2}{N} \tag{25}$$

$$SS\lambda_i = \frac{1}{nRc} \sum T_{..k.}^2 - \frac{T_{...}^2}{N} \tag{26}$$

$$SS(\alpha\beta)_{ij} = \frac{1}{nL} \sum T_{ij..}^2 - \frac{1}{nLc} \sum T_{i...}^2 - \frac{1}{nRL} \sum T_{.j.}^2 + \frac{T_{...}^2}{N} \tag{27}$$

$$SS(\alpha\lambda)_{ik} = \frac{1}{nc} \sum T_{i.k.}^2 - \frac{1}{nLc} \sum T_{i...}^2 - \frac{1}{nRc} \sum T_{..k.}^2 + \frac{T_{...}^2}{N} \tag{28}$$

$$SS(\beta\lambda)_{jk} = \frac{1}{nR} \sum T_{jk.}^2 - \frac{1}{nRL} \sum T_{j..}^2 - \frac{1}{nRc} \sum T_{.k.}^2 + \frac{T_{...}^2}{N} \tag{29}$$

$$SS(\alpha\beta\lambda)_{ijk} = \frac{1}{n} \sum T_{ijk.}^2 - \frac{1}{nL} \sum T_{ij..}^2 - \frac{1}{nc} \sum T_{i.k.}^2 - \frac{1}{nR} \sum T_{ijk.}^2 + \frac{1}{nLc} \sum T_{i..}^2 + \frac{1}{nRL} \sum T_{j..}^2 + \frac{1}{nRc} \sum T_{.k.}^2 - \frac{T_{...}^2}{N} \tag{30}$$

$$SS_{Error} = \sum X_{ijkl}^2 - \frac{1}{n} \sum T_{ijk}^2 \tag{31}$$

Where; $T_{...}$ = Grand sum

$T_{i...}$ = Sum of factor A at ith level

$T_{.j.}$ = Sum of factor B at jth level

$T_{..k.}$ = Sum of factor C at kth level

$T_{ij..}$ = Sum of interactions of A and B at ith and jth level

$T_{i.k.}$ = Sum of interactions of A and C at ith and kth level

$T_{.jk.}$ = Sum of interactions of B and C at jth and kth level

Note: $i = 1, 2, \dots, \dots, R$

$j = 1, 2, \dots, \dots, c$

$k = 1, 2, \dots, \dots, L$

$l = 1, 2, \dots, \dots, n$

Hence, to test for the significance of the factors A, B, and interaction effects, we use the Three way ANOVA table proposed below;

TABLE 4: THREE WAY CLASSIFICATION ANOVA

Source of Variance	Degrees of Freedom	Sum of Squares	Mean Squares	F-ratio
α_i	R-1	$SS\alpha$	$MS\alpha$	$MS\alpha/MSe$
β_j	c-1	$SS\beta$	$MS\beta$	$MS\beta/MSe$
λ_k	L-1	$SS\lambda$	$MS\lambda$	$MS\lambda/MSe$
$\alpha\beta$	(R-1)(c-1)	$SS\alpha\beta$	$MS\alpha\beta$	$MS\alpha\beta/MSe$
$\alpha\lambda$	(R-1)(L-1)	$SS\alpha\lambda$	$MS\alpha\lambda$	$MS\alpha\lambda/MSe$
$\beta\lambda$	(c-1)(L-1)	$SS\beta\lambda$	$MS\beta\lambda$	$MS\beta\lambda/MSe$
$\alpha\beta\lambda$	(R-1)(c-1)(L-1)	$SS\alpha\beta\lambda$	$MS\alpha\beta\lambda$	$MS\alpha\beta\lambda/MSe$
Error	RcL(n-1)	SSe	MSe	
Total		SST		

Therefore;

$$MS\alpha = \frac{SS\alpha}{R-1} \tag{32}$$

$$MS\beta = \frac{SS\beta}{c-1} \tag{33}$$

$$MS\lambda = \frac{SS\lambda}{L-1} \tag{34}$$

$$MS\alpha\beta = \frac{SS\alpha\beta}{(R-1)(c-1)} \tag{35}$$

$$MS\alpha\lambda = \frac{SS\alpha\lambda}{(R-1)(L-1)} \tag{36}$$

$$MS\beta\lambda = \frac{SS\beta\lambda}{(L-1)(c-1)} \tag{37}$$

$$MS\alpha\beta\lambda = \frac{SS\alpha\beta\lambda}{(R-1)(L-1)(c-1)} \tag{38}$$

4.3 Creep Experiments

Creep tests were conducted on the samples at a constant stress (loading) based on the average value of pressure obtained from, the operations data made available by Shell Production Development Corporation (SPDC), Bonga project, 130km off shore Nigeria, FPSO. The mean pressure is calculated at 14.1MPa (141bar). At applications of equations (1) to (10) in different combinations on the experimental field data, the true stress and strain tables were developed, thus;

TABLE 5: TRUE STRAIN VALUES

Sample A					
Temp/Time	1 hr.	1.5 hrs	2hrs	2.5 hrs	3hrs
50 °c	0.0140	0.0152	0.0162	0.0173	0.0175
70 °c	0.0193	0.0218	0.0221	0.0229	0.0234
90 °c	0.0256	0.0266	0.0283	0.0285	0.0288
110 °c	0.0269	0.0302	0.0330	0.0330	0
130 °c	0.0313	0.0352	0	0	0

Sample B					
Temp/Time	1 hr.	1.5 hrs	2hrs	2.5 hrs	3hrs
50 °c	0.0044	0.0099	0.0128	0.0139	0.0147
70 °c	0.0196	0.0208	0.0215	0.0222	0.0224
90 °c	0.0227	0.0229	0.0244	0.0251	0.0252
110 °c	0.0262	0.0280	0.0290	0.0298	0.0311
130 °c	0.0293	0.0309	0.0334	0	0

Sample C					
Temp/Time	1 hr.	1.5 hrs	2hrs	2.5 hrs	3hrs
50 °c	0.0045	0.0054	0.0073	0.0098	0.0099
70 °c	0.0190	0.0210	0.0214	0.0218	0.0220
90 °c	0.0198	0.0214	0.0222	0.0245	0.0259
110 °c	0.0222	0.0245	0.0264	0.0268	0.0290
130 °c	0.0274	0.0286	0.0305	0.0316	0.0331

Sample D					
Temp/Time	1 hr.	1.5 hrs	2hrs	2.5 hrs	3hrs
50 °c	0.0073	0.0078	0.0087	0.0091	0.0092
70 °c	0.0195	0.0199	0.0201	0.0203	0.0210
90 °c	0.0245	0.0256	0.0259	0.0264	0.0264
110 °c	0.0261	0.0271	0.0276	0.0286	0.0295
130 °c	0.0304	0.0312	0.0320	0.0326	0

Sample E					
Temp/Time	1 hr.	1.5 hrs	2hrs	2.5 hrs	3hrs
50 °c	0.0122	0.0150	0.0171	0.0177	0.0186
70 °c	0.0142	0.0156	0.0159	0.0174	0.0200
90 °c	0.0190	0.0197	0.0203	0.0208	0.0215
110 °c	0.0216	0.0224	0.0242	0.0273	0.0287
130 °c	0.0294	0.0306	0.0311	0.0331	0

Sample F					
Temp/Time	1 hr.	1.5 hrs	2hrs	2.5 hrs	3hrs
50 °c	0.0007	0.0012	0.0021	0.0030	0.0043
70 °c	0.0115	0.0122	0.0229	0.0149	0.0155
90 °c	0.0179	0.0183	0.0189	0.0191	0.0193
110 °c	0.0198	0.0207	0.0218	0.0256	0.0261
130 °c	0.0267	0.0278	0.0285	0.0320	0

TABLE 6: TRUE STRESS VALUES

Sample A x 10⁵ (Pa)

Temp/Time	1hr	1.5hrs	2hrs	2.5hrs	3hrs
50 °C	14.363	14.380	14.395	14.410	14.415
70 °C	14.440	14.476	14.481	14.492	14.500
90 °C	14.532	14.545	14.571	14.574	14.577
110 °C	14.551	14.598	14.640	14.668	0
130 °C	14.615	14.672	0	0	0

Sample B x 10⁵ (Pa)

Temp/Time	1hr	1.5hrs	2hrs	2.5hrs	3hrs
50 °C	14.226	14.304	14.345	14.361	14.373
70 °C	14.444	14.461	14.471	14.483	14.484
90 °C	14.488	14.506	14.514	14.525	14.526
110 °C	14.540	14.566	14.582	14.592	14.162
130 °C	14.585	14.409	14.646	0	0

Sample C x 10⁵ (Pa)

Temp/Time	1hr	1.5hrs	2hrs	2.5hrs	3hrs
50 °C	14.228	14.240	14.267	14.304	14.305
70 °C	14.436	14.464	14.470	14.475	14.479
90 °C	14.447	14.470	14.481	14.515	14.537
110 °C	14.482	14.515	14.543	14.549	14.580
130 °C	14.558	14.575	14.602	14.619	14.641

Sample D x 10⁵ (Pa)

Temp/Time	1hr	1.5hrs	2hrs	2.5hrs	3hrs
50 °C	14.267	14.274	14.285	14.295	14.296
70 °C	14.443	14.448	14.452	14.455	14.465
90 °C	14.515	14.531	14.537	14.542	14.577
110 °C	14.539	14.554	14.559	14.575	14.588
130 °C	14.602	14.612	14.625	14.634	0

Sample E x 10⁵ (Pa)

Temp/Time	1hr	1.5hrs	2hrs	2.5hrs	3hrs
50 °C	14.338	14.378	14.408	14.416	14.430
70 °C	14.366	14.386	14.389	14.413	14.450
90 °C	14.437	14.445	14.457	14.462	14.471
110 °C	14.472	14.485	14.510	14.557	14.578
130 °C	14.585	14.595	14.611	14.631	0

Sample F x 10⁵ (Pa)

Temp/Time	1hr	1.5hrs	2hrs	2.5hrs	3hrs
50 °C	14.174	14.181	14.194	14.206	14.223
70 °C	14.329	14.338	14.349	14.375	14.383
90 °C	14.421	14.426	14.435	14.437	14.438
110 °C	14.447	14.460	14.476	14.531	14.538
130 °C	14.547	14.559	14.574	14.625	0

Table 7a: Strains at various Temperatures for Sample A

Time (hr)	A ₅₀	A ₇₀	A ₉₀	A ₁₁₀	A ₁₃₀
1	0.0140	0.0193	0.0256	0.0269	0.0313
1.5	0.0152	0.0218	0.0256	0.0302	0.0352
2	0.0162	0.0221	0.0283	0.0330	0
2.5	0.0173	0.0229	0.0285	0.0350	0
3	0.0175	0.0234	0.0288	0	0

Table 7b: Strains at various Temperatures for Sample B

Time (hr)	B ₅₀	B ₇₀	B ₉₀	B ₁₁₀	B ₁₃₀
1	0.0044	0.0196	0.0227	0.0262	0.0147
1.5	0.0099	0.0208	0.0239	0.0280	0.0224
2	0.0128	0.0215	0.0244	0.0291	0.0252
2.5	0.0139	0.0222	0.0251	0.0298	0.0311
3	0.0147	0.0224	0.0252	0	0

Table 7c: Strains at various Temperatures for Sample C

Time (hr)	C ₅₀	C ₇₀	C ₉₀	C ₁₁₀	C ₁₃₀
1	0.0045	0.0190	0.0198	0.0222	0.0274
1.5	0.0054	0.0210	0.0214	0.0245	0.0286
2	0.0073	0.0214	0.0222	0.0264	0.0305
2.5	0.0098	0.0218	0.0245	0.0268	0.0316
3	0.0099	0.0220	0.0259	0.0290	0.0331

Table 7d: Strains at various Temperatures for Sample D

Time (hr)	D ₅₀	D ₇₀	D ₉₀	D ₁₁₀	D ₁₃₀
1	0.0073	0.0195	0.0245	0.0261	0.0304
1.5	0.0078	0.0199	0.0256	0.0271	0.0312
2	0.0087	0.0201	0.0259	0.0276	0.0320
2.5	0.0091	0.0203	0.0264	0.0286	0.0326
3	0.0092	0.0210	0.0264	0.0295	0

Table 7e: Strains at various Temperatures for Sample E

Time (hr)	E ₅₀	E ₇₀	E ₉₀	E ₁₁₀	E ₁₃₀
1	0.0122	0.0142	0.0190	0.0216	0.0294
1.5	0.0150	0.0156	0.0197	0.0224	0.0306
2	0.0171	0.0159	0.0203	0.0242	0.0311
2.5	0.0177	0.0174	0.0208	0.0273	0.0331
3	0.0186	0.0200	0.0215	0.0287	0

Table 7f: Strains at various Temperatures for Sample F

Time (hr)	F ₅₀	F ₇₀	F ₉₀	F ₁₁₀	F ₁₃₀
1	0.0007	0.0115	0.0179	0.0198	0.0267
1.5	0.0012	0.0122	0.0183	0.0207	0.0278
2	0.0021	0.0129	0.0189	0.0218	0.0285
2.5	0.0030	0.0149	0.0191	0.0256	0.0320
3	0.0042	0.0155	0.0193	0.0261	0

4.2.1 Creep Curves

The creep experiments were conducted under constant stress (load) which produced varying strain effects on different samples at various temperatures and time intervals. The strain-time curves shown below portray the effect of creep on the samples of study which were taking from Tables 7a-to-7f.

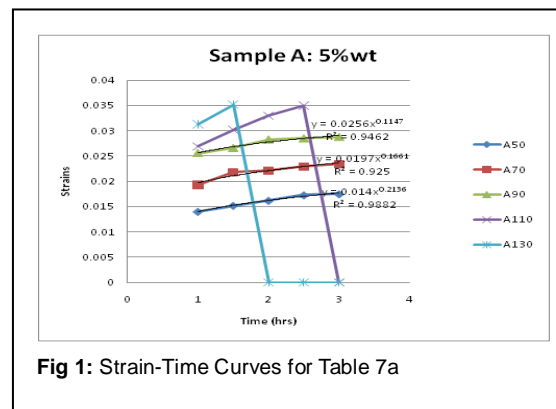


Fig 1: Strain-Time Curves for Table 7a

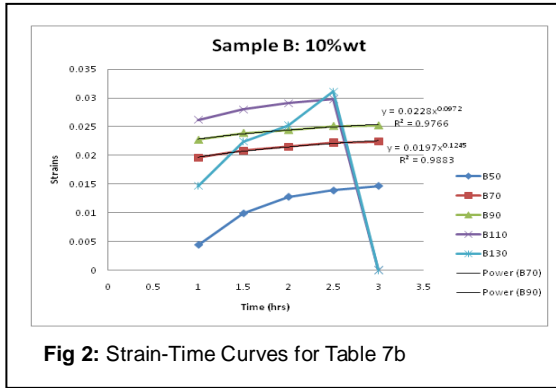


Fig 2: Strain-Time Curves for Table 7b

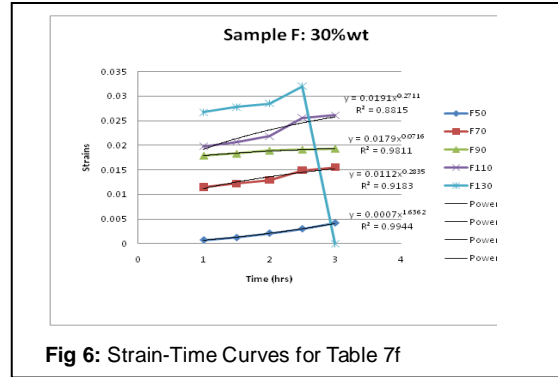


Fig 6: Strain-Time Curves for Table 7f

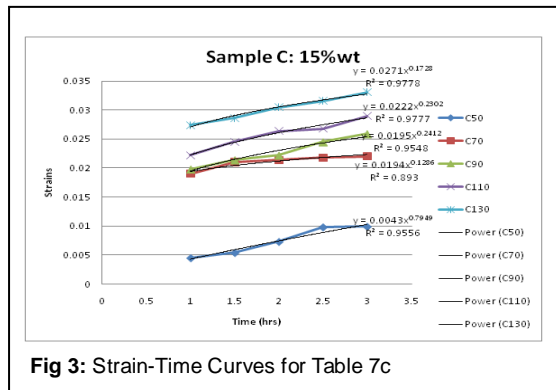


Fig 3: Strain-Time Curves for Table 7c

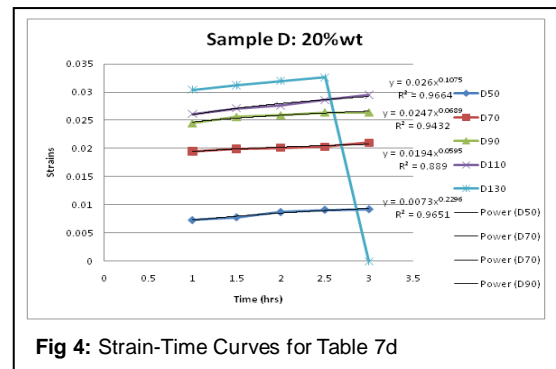


Fig 4: Strain-Time Curves for Table 7d

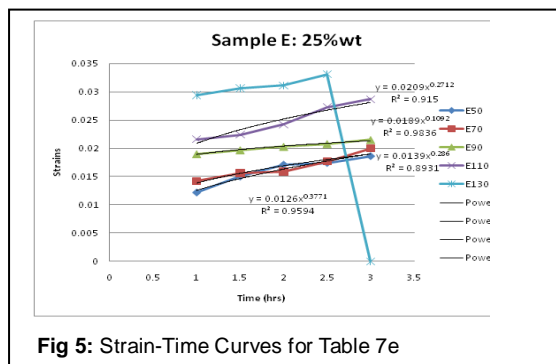


Fig 5: Strain-Time Curves for Table 7e

5 ANALYSIS OF DATA USING SPSS SOFTWARE

The true strain and stress data generated in this research can further be analyzed to investigate the variance between samples and the significant effect of factors and treatments. The “SPSS” statistical tool is employed to this regard by applying: One way, Two way and further Three way classification analysis of variance, nonetheless, the One way analysis produced no significant result hence its details were ignored. The results of the analysis are shown in the following tables below, while the details are in Appendix C. The level of significance adopted throughout the analysis of this research data is 95 percent confidence interval, making our significance level to 0.05. Due to the bulky nature of the data collected, the manual computation will be too cumbersome and full of analytical mistakes so, the use of statistical software was advised. The software used for this analysis as earlier mentioned is SPSS (Statistical Package for Social Sciences) version 17. The collected field data (experimental data) were reduced to a one observation per cell to depict creep parameters (strain and stress) of the samples. The statistical inference drawn from the analysis is based on the following null hypotheses and their alternatives;

1. H0: The main effects (time, temperature, and sample) are not significant.
2. H1: The main effects are significant.
3. H0: The interaction effects are not significant.
4. H1: The interaction effects are significant.

The ANOVA tables that follow are drawn from analysis done with SPSS software .

TABLE 8: SPSS – TWO WAY ANOVA FOR DEPENDENT VARIABLE STRAIN

Source	Type III Sum of Squares	df	Mean Square	F	Sig.
Corrected Model	.001 ^a	8	.000	1.248	.335
Intercept	.011	1	.011	100.099	.000
Temp.	.001	4	.000	1.536	.239
Hours	.000	4	.000	.959	.456
Error	.002	16	.000		
Total	.014	25			
Corrected Total	.003	24			

TABLE 9: SPSS – TWO WAY ANOVA FOR DEPENDENT VARIABLE STRESS

Source	Type III Sum of Squares	df	Mean Square	F	Sig.
Corrected Model	398.590 ^a	8	49.824	2.573	.051
Intercept	3718.438	1	3718.438	192.004	.000
Temp.	118.331	4	29.583	1.528	.028
Hours	280.258	4	70.065	3.618	.241
Error	309.864	16	19.366		
Total	4426.891	25			
Corrected Total	708.453	24			

From Tables 8 and 9, it is obviously inferred that the Two way classification could not produce the interaction effect, even the temperature and time (hour) effects are not significant for the Strain variable (table 8), but temperature showed a good significant effect on the samples in the case of Stress variables (table 9). The ANOVA for sample C (strain) indicates that time (hour) and temperature treatments are super significant on the material sample C. Only temperature treatment showed significant effect on sample D and also on sample F and slight significance on sample B. The ANOVA of dependent variable Stress also produced the facts that temperature treatment showed a significant effect on sample A unlike in strain. A super significance is observed for both time and temperature treatments on sample C, a slight significance of temperature on sample B but no significant of both temperature and time treatments on rest of the samples. As stated earlier no interaction effects were recorded in the analysis for both Stress and Strain variables. The actual reason for this development (no sign of interaction effect) is because the data have only one observation per cell, hence no interaction effect came out of the analysis, as this has been reduced to the error or residual in the model. Also, there was no sample effect since the analysis was two way accommodating only temperature and time effects. Then, we move a step further to the three way classification of analysis of variance to search for both sample and interaction effects.

TABLE 10: SPSS – THREE WAY ANOVA FOR DEPENDENT VARIABLE STRAIN

Source	Type III Sum of Squares	df	Mean Square	F	Sig.
Corrected Model	.010 ^a	69	.000	4.359	.000
Intercept	.062	1	.062	1875.218	.000
Sample	.001	5	.000	3.369	.008
Hour	.000	4	7.364E-5	2.236	.072
Temperature	.004	4	.001	31.942	.000
Sample-Hour	.001	20	3.170E-5	.962	.514
Sample-Temperature	.002	20	8.815E-5	2.676	.001
Hour-Temperature	.002	16	.000	4.651	.000
Error	.003	80	3.294E-5		
Total	.074	150			
Corrected Total	.013	149			

Due to full factorial nature of the design (that is no error term) the interaction effect was used as error (effect of single observation per cell). Therefore, at two way, no interaction effect was estimated but at three way the two way interaction was drawn but not three way interaction because the three way interaction was used as error. The statistical inferences drawn from Table 10 above on the strain variable are;

1. Sample effects are significant.
2. Hour (time) effects are not significant.

3. Temperature effects are super significant.
4. Sample-hour interaction effects are not significant.
5. Sample-temperature interaction effects are very significant.
6. Hour-temperature interaction effects are super significant.

TABLE 11: SPSS – THREE WAY ANOVA FOR DEPENDENT VARIABLE STRESS

Source	Type III Sum of Squares	df	Mean Square	F	Sig.
Corrected Model	1312.496 ^a	69	19.022	3.303	.000
Intercept	27752.433	1	27752.433	4818.668	.000
Sample	75.970	5	15.194	2.638	.029
Hour	170.977	4	42.744	7.422	.000
Temperature	318.107	4	79.527	13.808	.000
Sample-Hour	97.470	20	4.874	.846	.652
Sample-Temperature	185.351	20	9.268	1.609	.071
Hour-Temperature	464.620	16	29.039	5.042	.000
Error	460.749	80	5.759		
Total	29525.677	150			
Corrected Total	1773.244	149			

The statistical inferences drawn from Table 11 on the stress variable are;

1. Sample effects are significant.
2. Hour (time) effects are super significant.
3. Temperature effects are super significant.
4. Sample-hour interaction effects are not significant.
5. Sample-temperature interaction effects are not significant.
6. Hour-temperature interaction effects are super significant.

5.1 FURTHER ANALYSIS OF RESULTS AND INFERENCES

5.1.1 Material Strength

From Table 2, it is apparent that the new hybrid nanocomposite material has high strength compared to the baseline epoxy-alumina nanocomposite material. The new hybrid material with a 15%wt fraction of fillers (13%wt. alumina and 2%wt. calcium silicate) showed the highest tensile strength of 90Mpa followed by the new hybrid material with a 20%wt. fraction of fillers, which has a tensile strength of 84Mpa. Nevertheless, the baseline nanocomposite material with a 30%wt. fraction of alumina filler showed a good strength of 83Mpa.

5.1.2 Strain-Time Creep Curve

The curves of Fig.1 to Fig.6 show the creep response of each hybrid nanocomposite basically at the secondary creep stage. The creep curves obey the power law of the following form;

$$\epsilon = At^n \tag{39}$$

The equation above depicts the strain-time relationship which governs all the line equations of the creep curves (Figures 1 – 6). Through these line equations the time (t) of failure for the uncreeped materials can be predicted. The correlation coefficients of these lines are also shown on the graphs.

5.2.3 The ANOVA Post Hoc Tests and Inferences

This is the post ANOVA tests for make multiple comparisons for the main effects (samples, time and temperatures), among each effect, basically carried out after the three way classification analysis, as it is the only

analysis that shows the interaction effect. Post hoc tests for the dependent variable strain produced the following results; It is clearly observed in the comparisons between samples according to the mean difference, that sample C showed superior means over other samples except sample D. This indicates that samples C and D are the best of the new hybrid nanocomposites, which is in affirmation with the result obtained on the tensile tests. In terms of hour (time) comparisons, the third hour (3 hrs) is the only time with remarkable significance when compared with others, which shows that samples were mostly affected at this period. Finally, the 50 degrees temperature shows a super significance over others, this means that all the samples will operate best at this temperature. Post hoc tests for the dependent variable stress produced the following results; Sample C at this instant also showed superior means over other samples, followed closely by sample D. This also confirms the previous inferences drawn from the strain and tensile tests. Multiple comparisons on time indicate also that stress is most significant at the third hour (3 hrs) just as in the case of strain. But the post hoc tests for temperature at stress variable shows that stress is most significant at 130 degrees temperature than at any other temperature.

6 CONCLUSION

The high temperature creep and creep fracture properties of engineering materials are usually analyzed in terms of the variations in minimum creep rate and rupture life, with stress and temperature. In this research we applied an experimental design in collection of the field data and further application of analysis through standard statistical software. The strength of the new hybrid nanocomposite material was measured using a dependable tensile testing machine. The result of the tensile test shows that the new hybrid composite material has good strength when compared with the strength of a neat epoxy or the baseline epoxy/alumina composite material. The development of the creep testing machine is another phase of this research work which we did not lay emphasis upon but nonetheless, made good contribution towards the actualization of this research work. Creep experiment which was used in generating the required field data (elongation) for the research helped on provision of the required stress-strain data through the application of some analytical models. The short term creep experiment conducted at constant stress but at varying temperatures and time, shows the new hybrid materials creep response at various temperatures and time. Each of the new materials showed good creep resistant property at temperatures between 500C and 900C but the 15%wt and 20%wt filler constituent exhibited good creep resistance above these temperatures. The hybrid composite with 15%wt constituent was the only one that could withstand temperature of 1300C.

REFERENCES

1. Akita, H., and Hattori, T. (1999). Studies on molecular composite.I. Processing of molecular composites using a precursor polymer for poly(P-Phenylene benzobisthiazole). *Journal of Polymer Science: Part B: Polymer Physics*, 37(3), 189-197.
2. ASM International (n.d). Tensile testing:. Introduction to tensile testing (2nd ed).www.asminternational.org.
3. Athawale, A.A., Bhagwat, S.V., Katre, P.P., Chandwadkar, A.J., and Karandikar, P. (2003). Aniline as a stabilizer for metal nanoparticles. *Materials Letters*, 57(24-25),3889-3894.
4. Daniel, I.M., Miyagawa, H., Gdoutos, E.E., and Luo, J.J. (2003). Processing and characterization of epoxy/clay nanocomposites. *Express Mechanics*, 43, 348 – 354. Doi: 10.1243/03093247V293159.
5. Endo, M., Naguchi, T. and Ho, M., (2008). Extreme – performance rubber nanocomposites for probing and excavating deep oil resources using multi walled carbon nanotubes. *Advanced Functional Materials*, 18, 3403 -3409.
6. Evora, V.M.F., and Shukla, A. (2003). Fabrication, characterization and dynamic behaviour of polyester/TiO2 nanocomposites. *Material Science Engineering A*, 36, 358 – 366.
7. Eze, F.C.(2002). Introduction to analysis of variance, volume 1. Obiagu, Enugu: Lanno.
8. Gedney, R. (2002). Guide to testing metals under tension. *Advanced Materials and Processes*, pp 29 – 31.
9. Gojny, F.H., Wichmann, M.H.G., Kopke, U., Fiedler, B., and Schulte, K. (2004). Carbon nanotube reinforced epoxy – composites: Enhanced stiffness and fracture toughness at low nanotubes content. *Composite science and Technology*, 64, 2363 – 2371: Elsevier. Retrieved from <http://www.hinari-gw.who.int/composite science technology>.
10. Gorga, R.E., and Cohen, R.E. (2004). Toughness enhancements in poly (methyl methacrylate) by addition of oriented multi-wall carbon nanotube. *Journal of Polymer Science, Part B: Polymer Physics*, 42(4), 2690-2702.
11. Jenkins, M.G. (2007). *Mechanical Engineering: Me 354 [Lecture notes]*. Seattle, Washington: University of Washington, Department of Mechanical Engineering.
12. Lea, R.H. (2002). Composite piping systems to improve celi and gas production. Baton Ronge, LA: Edo Specialty plastics.
13. Luo, J.J., Daniel, I.M. (2003). Characterization and modeling of mechanical behaviour of polymer/clay nanocomposites. *Composite Science and Technology*, 63(11), 1607-1616.
14. Masahiro, K., Yoshimichi, O., Masanori, K., Shigemitsu, O., and Toshikalsu, T. (2006). Preparation and various characteristics of

- epoxy/alumina nanocomposites. *IEEJ Transactions on Fundamentals and Materials*, 126 (11), 1121 – 1127: The Institution of Electrical Engineers of Japan. Doi:10.1541/ieejfms.126.1121.
15. Meda, L., Marra, G., Galfetti, L., Inchingalo, S., Severini, F., na De Luca, L. (2005). Nanocomposites for rocket solid propellants. *Composites Science and Technology*, 65(5), 769-773.
 16. Milue, D. (2000). Small solutions for big returns. *Oil and Gas Next Generation*, Q4, 2009, 93-98. Retrieved from <http://www.ngoilgas.com>.
 17. Omrani, A., Simon, L.C., and Rostami, A. (2009). The effect of alumina nanoparticle on the properties of epoxy resin system. *Materials Chemistry and Physics* 114 (1), 145 – 150: Elsevier. Retrieved from <http://www.hinari-gw.who.int/compositescience>.
 18. Oriakhi, C.O. (1998). Nano Sandwiches. *Chemical Briefing*, 34:59-62.
 19. Park, C., Park, O., Lim, J., and Kim, H. (2001). The fabrication of syndiotactic polystyrene/organophilic clay nanocomposites and their properties. *Polymer Letters*, 42, 7465 -7475.
 20. Ray, S.S., and Bousmina, M. (2005). Brodegradable polymers and their layered silicate nanocomposites: In greening the 21st century materials world. *Progress in Materials Science*, 50(8), 962-1079.
 21. Ritchie, R.O. (1993). Mechanical behavior of materials [Lecture notes]. Rhoads, Berkely, California: University of California.
 22. Roy, R., Roy, R.A., and Roy, D.M. (1986). Alternative perspectives on quasi-crystallinity: non-uniformity and nanocomposites. *Material Letters*, 4 (8-9), 323 – 328.
 23. RTO Lecture series, EN-AVT- 129, May 2005.
 24. Sailor, M.J., and Link, J.R. (2005). Smart dust: Nanostructured devices in a grain of sand. *Chemical Community*, 2005, 1375-1383.
 25. Schmidt, D., Shah, D., and Giannelis, E.P. (2002). New advances in polymer/layered silicate nanocomposites. *Current opinion in solid and Materials Science*, 6 (3), 205 – 212.
 26. Scott, S., Crudden, C.M., and Jones, C. W. (Eds) (2003). Nanostructured catalysts. *Nanostructure science and Technology Series*, P.342. New York: Springer.
 27. Seppala, J. (2010). Editorial corner – a personal view Nanocomposites, excellent properties or hype? *eXPRESS Polymer Letters*, 4 (3), 130. DOI: 3144/expresspolymlett.2010.17
 28. Usuki, A., Kawasum, M., Kojima, Y., Okada, A., Kuraruchi, T., and Kamigaito, O.J. (1993). Swelling behaviour of Montmorillonite cation exchanged for v-amiro acids by E-caprolactam. *Materials Resources*, 8(5), 1174.
 29. Vincenzo, S., Fallatah, G.M., and Mehdi, M.S. (2010). Applications of nanocomposite materials in the Oil and Gas industry. *Advanced Materials Research*, 83(86), 771-776.
 30. Walpole, R. E. (1982). *Introduction to statistics* (3rd ed.)pp 403 – 428. New York: Macmillan.
 31. Wilshire, B., and Evans, R.W.(1994). Acquisition and analysis of creep data. *The Journal of Strain Analysis for Engineering Design*, 29, 159 – 165.
 32. Yong, V., and Hahn, H.T (2004). Processing and properties of SiC/Vinyl ester nanocomposites. *Nanotechnology*, 15, 1338-1343.
 33. Zavyalov, S.A., Pivkina, A.N., and Schoonman, J. (2002). Formation and characterization of metal-polymer nanostructured composites. *Solid State Ionics*, 147(3-40), 415-41.